Barium cerate and its composite perovskites – synthesis techniques: a comprehensive review

Seere Valappil Jasira[1], Vannadil Puthiyaveetil Veena[1], Cherlan Kottianmadathil Shilpa[1], Kavukuzhi Meerasahib Nissamudeen[1]*

[1]Department of Physics, Kannur University, SAT Campus,
Edat, Payyanur, 670327

*Corresponding author: K M Nissamudeen, nisamkm@kannuruniv.ac.in, +91-9387838499

Abstract

Perovskites have attracted growing interest in recent eras due to their unique properties and potential applications. Barium cerate (BC) proton-conducting perovskites have been examined over decades for various applications such as hydrogen sensors, fuel cells, proton separation membranes, etc. When compared with oxide ion conductors under the same circumstances, ceramic proton conducting barium cerate can diminish the working temperature of solid oxide fuel cells to an intermediate temperature range, 673 – 873 K because of their higher ionic conduction. The present review carefully analyses and summarizes different synthesis approaches with optimization conditions to prepare BC-derived perovskites and the reported data have been carefully analyzed. A range of synthesis methods such as solid-state reaction method and wet chemical processes like coprecipitation, combustion, Pechini method, etc., have been systematically investigated. Even though the solid-state method has considerable disadvantages, most researchers avoid its incompetence due to the easiness of processing. Applications of the material have been briefly deliberated to exemplify its technological importance. The present review concluded with the recent signs of progress and innovative techniques employed to overcome the processing complications in these materials.

Keywords: barium cerate, perovskite, SOFC, proton conduction, review

1. Introduction

Solid Oxide Fuel Cell (SOFC) is an ecological device that transforms chemical bond energy into valuable electrical energy with effective means. Generally, there exist three types of SOFC: low temperature (≤ 723 K), intermediate temperature (773 – 1023 K), and high

temperature (873-1273 K). In this class, productive and effective SOFCs are high-temperature ones. But their use is mostly restricted due to the exploitation of materials at high temperatures. Therefore, reducing the working temperature to an intermediate level with negligible electronic conductivity, satisfactory mechanical strength [1], consistent productivity and effectiveness is a most pertinent question. So, developing innovative materials with fascinating thermal, physical, and conducting properties is a necessity [2].

The major components of SOFCs are electrodes (anode and cathode) and electrolytes. At the working temperature, the electrolyte should satisfy certain conditions such as low electronic conductivity, high ionic conductivity, thermal, physical, and chemical stabilities under an oxidizing and reducing atmosphere. Currently, the main electrolytes include co-doped ceria, lanthanum silicate apatite, Ba-Zr and Ba-Ce mixed oxides, molybdenum oxides, yttria-stabilized zirconia (YSZ) etc. Normally, the active components in SOFCs are complex oxide materials having a perovskite phase with high ionic conductivity. Perovskites are employed to develop every part of SOFC: as an anode, cathode, and electrolyte material [2].

In 1981, proton-conducting oxide perovskites were first investigated by Iwahara *et al*., who predicted its potential usage as an electrolyte in various applications extending from hydrogen pumps to fuel cells. Subsequently, a wide range of aliovalent metal ions doped zirconates, titanates, and cerates have been described and their structural, physical, chemical and electrical properties have been studied [3]. Among the perovskite materials, barium cerate is of particular interest. BC perovskites can be efficiently used as an electrolyte for intermediate-temperature solid fuel cells [2]. Fig. 1 highlights the number of papers published over the past years on BC perovskites for SOFC application. Depending on the type of fuel cell, ionic motion in the electrolyte can be either the positive ions (H^+) drifting towards cathode or negative ions (O^{2-}) drifting towards anode. In doped BC perovskites, the leading conduction mechanism may vary from protonic to oxide in the temperature range of 873 to 1273 K [4]. Here water reacts with oxygen vacancies in a humid atmosphere to generate proton carriers at low temperatures. Whereas at higher temperatures, the water splits into hydrogen and oxygen ions and the conductivity is regulated by O^{2-} ions [5, 6].

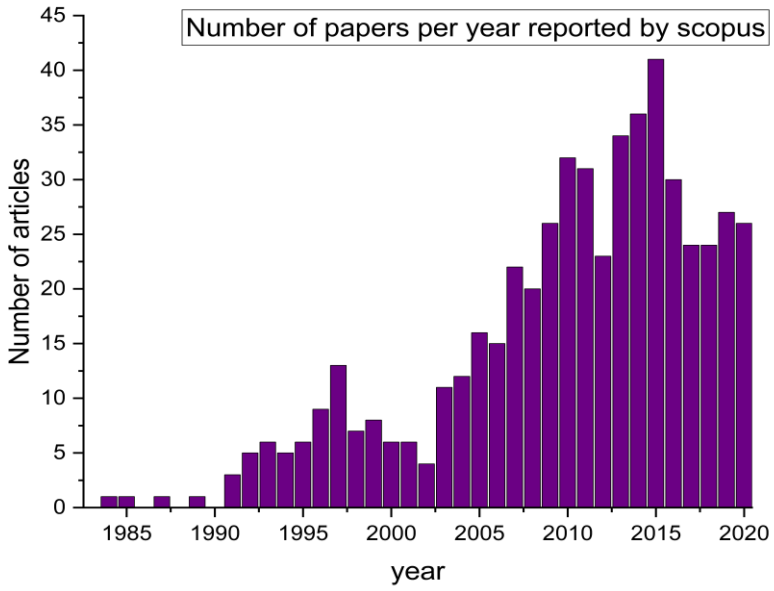

Fig. 1 Number of research articles published per year as per Scopus, searching for ‘‘barium cerate’’ in their abstracts, titles or keywords.

The crystal phase of BC has been described as tetragonal, orthorhombic, monoclinic, or cubic. Doped and undoped BC crystal perovskite belongs to the distorted perovskite structure ($GdFeO_3$ structure). To boost bulk and grain boundary conductivity, doping with other elements is normal. The addition of trivalent ions in the site of quadrivalent ions, *ie*, replacing Ce^{4+} with Y^{3+}, Gd^{3+}, and others creates vacancies in oxygen sites or creates electronic holes in an oxidizing atmosphere. Exposing this compound to a hydrogen /water-containing atmosphere may cause hydroxyl groups to occupy former vacancies in oxygen sites, which enhances protonic conductivity at intermediate temperatures. By placing these compounds into the extremely high oxidizing atmosphere, an interchange of electronic holes with protons will take place [7]. When doped with RE^{3+} ions, BC crystal shows a very slight change in the structure due to a similar ionic radius of RE^{3+} ions with cerium ion [4]. Distorted perovskite materials often undergo phase shifts to advanced symmetric phases upon heating. The same has been suspected for barium cerate too, but its existence looks to be tough due to desperately controllable investigational constraints such as oxygen content, humidity, etc. [4].

Doping elements with high ionic sizes than Ce^{4+} enhance the protonic conductivity of barium cerate, whereas dopants with higher electronegativity enhance chemical stability. The greatest protonic conductivity in BCs and zirconates was seen in the case of doping with yttrium, following gadolinium, and then by other lanthanide elements like Pr and Yb which

show mixed electronic and ionic conduction. An evaluation of electronegativity and ionic conductivity recommends that both yttrium and gadolinium appear to be the optimal doping for the Ce site in barium cerate. Also "mean-field approach" computational studies show that the smallest energy solutions are obtained for Y and Gd doping [7].

The impact of the production methods on the electrical and structural characteristics of SOFC materials is fetching more and more significance, especially when nanomaterials having higher quality are essential [8]. In view of the above, an attempt is made to gather different synthesis methods to prepare BC perovskites with a brief analysis.

2. Preparation methods of barium cerate-based materials

In 1981, Iwahara *et al*., introduced BC perovskites for application in proton conduction. There are different methods to synthesize BC derivative compounds which could be divided into solid-state reaction synthesis (calcination of a mixture of oxides of reactant material) and wet chemical methods (preparation from solutions) [9]. The impact of preparation methods on various properties of materials used for SOFCs is fetching more and more significance, particularly when nanoceramics of superior excellence are essential [8, 10]. Hence a thorough investigation of different methods used to synthesize various barium-cerium compounds has much more importance. A variety of different methods used to synthesize BC perovskites are discussed below.

2.1 Solid-state synthesis

The solid-state reaction method is the most communal method for preparing oxide perovskites. BC and its derivatives were first synthesized by the solid-state reaction method. In this process, a stoichiometric amount of precursor metal carbonates or oxides is ground using mortar / ball-mill and dried, then calcined at a specific high temperature to obtain oxide perovskite powder. This method is a promising process for bulk synthesis owing to its simple procedure, but the homogeneity of the resulting product is poor, ensuing in a lower purity [6].

Virkar *et al*., (1982) prepared pure and yttrium-doped BC with calcination temperatures of 1373 K and 1523 K respectively for four hours. Here barium carbonate, cerium oxide and yttrium oxide were taken in stoichiometric proportion. They compared the electrical conductivity of different dopant concentrations and found that conductivity increases with an increase in dopant concentration up to 10 m/o and then remains constant [11].

Nd-doped BC ($BaCe_{0.9}Nd_{0.1}O_{3-\alpha}$) was prepared by Chen *et al*., (1997) through a solid-state reaction route using the ball-milling method (COB) and mortar/pestle method (COM). A stoichiometric mixture of reactants was ball milled for 36 h in ethanol. The resulting mixture was desiccated at room temperature and calcined in air at 1573 K for 10 h. The powder was then ground and ball-milled using ethanol for 4 h to get a powder sample. In the mortar route, the initial chemicals were ground using mortar for 30 minutes. This mixture was heated from 298 K to 1673 K at a rate of 20 K min^{-1}. It is then calcined at 1573 K. The calcinated powder is again ground using mortar to get a fine powder. XRD analysis of both powders showed that at above 1273 K, only a single-phase crystal was formed. Powder from COB has less particle dimension, huge surface area, and homogeneous particles whereas COM has a small surface area, big particle dimension, and some agglomerates also [12].

Later in 2005 Pelletier *et al*., studied doped BC ($BaCe_{0.8}Gd_{0.2}O_{3-\alpha}$ and $BaCe_{0.8}Gd_{0.19}Pr_{0.01}O_{3-\alpha}$). They used a stoichiometric ratio of high purity chemicals, mixed, ground, and ball-milled using isopropyl alcohol for about 24 hours. This dry mixture was calcinated for 10 h at 1623 K to get the final perovskite structure. This powder was converted into pellets that were used in ammonia fuel cells. The performance of fuel cells using BCGP electrolytes was improved by about 40% over BCG electrolytes in either H_2 or straight ammonia feed [13]. In the same year, Zolkos *et al*., systematically studied the calcination temperature needed for the conventional solid-state reaction method to prepare BC perovskite and also studied the transition metal cation effects on the preparation process, properties, and morphology of the material. They varied the temperature of calcination from 1273 K to 1573 K in 100 K intervals. When calcinated at 1273 K, barium carbonate and ceric oxide phases were found along with the BC phase. Above 1373 K, only the BC phase was found. At above 1573 K, particle dimension ranging from 5 to 20 µm was obtained. Metal doping had a significant effect on the size of particles and the sinterability of the material. Doping Nd resulted in particle size reduction and Mn doping increases the particle size and perovskite sinterability [14].

Przybylski *et al*., (2011) prepared $BaCe_{0.7}In_{0.3}O_{2.85}$ (BCI30) and studied these along with other compositions in the atmosphere consisting of N_2, CO_2, and H_2O in various ratios and various temperatures (298 – 873 K). BCI 30 particles had 500 nm grain size. From the SEM image, some huge aggregates were visible in BCI 30 [15]. Pulphol *et al*., (2019) explored the consequence of reducing atmosphere on different physical properties of pure and Nb-incorporated BC. Samples were calcined at 1373 K for 10 h and sintered at 1873 K for 5h.

Then annealed in a mixture of hydrogen and argon at various temperatures to find out the consequences. At least up to 1723 K, the BC sample was found to be thermodynamically stable upon annealing in a reduced atmosphere. The sample decomposed at 1823 K. Greater annealing temperature produced higher Ce^{3+} ion concentration and greater electrical conductivity. By increasing the annealing temperature from 1573 to 1723 K, the activation energy of conductivity reduced from E_a = 0.31 to 0.263 eV in reduced Ar [16].

Recently Zvonareva *et al*., (2021) investigated $BaCe_{0.8-x}Sn_xYb_{0.2}O_{3-\alpha}$ prepared using $BaCO_3$, SnO, CeO_2, and Yb_2O_3 as initial reactants. Stochiometric amounts were mixed in an agate mortar with acetone and calcinated the mixture at 1273 K for 8 h. 0.5wt% CuO as a sintering aid was added into the powder and calcined at 1173 K for 1 h. After grinding and milling and further calcination at 1773 K, got a ceramic sample. XRD pattern showed that all compositions were found to be single-phased with cubic perovskite structure. The incorporation of tin resulted in a decrease in the basicity and lattice parameters of complex oxides. As a consequence, conductivity was reduced over the whole range of examined oxygen and vapor partial pressure values. However, these materials are considered suitable materials for proton-conducting electrolyte application in SOFCs due to their respectable chemical stability and ionic conductivity [17]. The preparation conditions and basic characteristics of powders obtained from the solid-state reaction method are summarized in table 1.

Composition	calcination temperature and time (K, h)	Sintering temperature and time (K, h)	mixing technique used, mixing solvent	structure	reference
$BaCeO_3$	1523, 4 in Pt	1623/4	acetone	single phase	[11]
$BaCeO_3$: Y	1373, 4 in Pt	1623/4	acetone	single phase	
$BaCe_{0.9}Nd_{0.1}O_{3-\alpha}$	873 – 1573, 10	1473-1673/10 or 1773/2	ball milling (36h), ethanol	single-phase > 1273 K	[12]
$BaCe_{0.9}Nd_{0.1}O_{3-\alpha}$	873 – 1573, 10	not sintered	agate mortar (30 min)	single-phase > 1273 K	
$BaCe_{0.8}Gd_{0.2}O_{3-\alpha}$, $BaCe_{0.8}Gd_{0.19}Pr_{0.01}O_{3-\alpha}$	1623, 10	1873/10	ball milling (24 h), isopropyl alcohol	*	[13]
$BaCeO_3$, $BaCe_{0.99}Nb_{0.01}O_3$	1373, 10	1873, 5	ball milling 20 h, ethanol	orthorhombic	[16]
$BaCe_{0.8-x}Sn_xYb_{0.2}O_{3-\alpha}$ (with addition of CuO)	1273, 8 and 1173, 1	1773, 5	agate mortar, acetone	cubic	[17]
$BaCe_{1-x}Gd_xO_{3-x/2}$	1373 and refiring at 1673, 10	1748/10	ball milling	cubic	[18]
$BaCe_{1-x}Gd_xO_{3-\alpha}$	1673, 2	1873/3	agate mortar/1 h, ethanol	orthorhombic	[18, 19]
$BaCe_{0.99-x}Gd_xCu_{0.01}O_{3-\alpha}$	1423, 2	1723/3	agate mortar/1 h, ethanol	orthorhombic	
$BaCe_{0.9-y}Gd_{0.1}Cu_yO_{3-\alpha}$	1423, 2	1723/3	agate mortar/1 h, ethanol	orthorhombic	[19]

$BaCe_{1-x}Zr_xO_3$	1623, 6 in alumina	1773, 10	agate mortar for an hour and ball milling, isopropyl alcohol	orthorhombic	[20]
$BaCe_{0.5}Nb_{0.5}O_3$	1273-1473	1473-1673, 4-6	ball milling, acetone	cubic	[21]
$BaCeO_3$	1273	1773	*	orthorhombic	[22]
$BaCeO_3$: Bi	1273 – 1473, 10-12	1473, 10-12	*	*	[23]
$BaCeO_3$	1673, 4	1473, 10-12	*	*	[24]
$BaCeO_3$	1523, 4 in Pt	1623,4	*	*	
$BaCeO_3$: Y	1373, 4 in Pt	1623, 4	*	*	
$BaCeO_3$: Yb	1273, 48 in alumina	1623, 96	*	*	
$BaCeO_3$: Ca, Eu, Gd, Nd, Yb	1523, 5 in alumina	1773, 12	*	*	
$BaCeO_3$: Yb, Y, Gd, La	1273, 6	1723, 96	*	*	
$BaCeO_3$: Ho, Nd, La	1373, 4 in Pt	1623, 4	acetone	*	[25]
$BaCeO_3$: Nd, La, Y, Ca	1523, 5 in air	1773, 10	*	orthorhombic	[26]
$BaCeO_3$: Gd, La, Nd, Y, Yb	1523, 15 in alumina	1773, 10	*	cubic	[27]
$BaCe_{0.95}Y_{0.05}O_{3-\alpha}$, $BaCe_{0.9}Gd_{0.1}O_{3-\alpha}$	1523, 15 in alumina	1773, 10	dry mixing	cubic	[28]
$BaCe_{0.9}Y_{0.1}O_{2.95}$, $BaCe_{0.9}Gd_{0.1}O_{2.95}$	1773, 20	Not sintered	ball milling	orthorhombic and tetragonal	[29]
$BaCeO_3$: Nd, Gd, Yb	1523-1673, 5-14 in alumina	1773, 12	*	orthorhombic	[30]
$BaCeO_3$: Y	1373, 10 in alumina	1723, 40	ball milling	*	[31]
$BaCe_{0.85}Gd_{0.15}O_{3-\alpha}$ and $BaCe_{0.9}Gd_{0.1}O_{3-\alpha}$	1523, 12	1923, 10-12	ball milling	single phase	[32]
$BaCe_{0.9}Y_{0.1}O_{3-\delta}$	1573, 10 in alumina	1823, 10	planetary mill, 3h, acetone	*	[33]
$BaCe_{1-x}Y_xO_{3-x/2}$	1723	1723	agate mortar, 10 min	orthorhombic	[34]
$BaCe_{0.8}Gd_{0.2}O_{3-\delta}$	1623, 10	1873, 10	ball milling, 24 h, isopropyl alcohol	single phase	[35, 36]
$BaCe_{0.8}Gd_{0.2-x}Pr_xO_3$	1623, 10	1873, 10	ball milling, 24 h, isopropyl alcohol	orthorhombic	[37]
$BaCeO_3$:In	1373, 2, and 1573, overnight	1673, 12	ball milling, 1 h, and planetary milling, 2h	orthorhombic	[38]
$BaCe_{0.8}Gd_{0.15}Pr_{0.05}O_{3-\delta}$, $BaCe_{0.85}Sm_{0.15}O_{3-\delta}$, $BaCe_{0.85}Eu_{0.15}O_{3-\delta}$	1623, 10	1773, 12	ball milling, 24 h, isopropyl alcohol	cubic	[39]
$BaCe_{1-x}Nb_xO_{3-\alpha}$	1173, 12 in alumina	1773, 24	ball milling, 6h, 2-propanol	cubic	[40]
$BaCe_{0.9-x}Zr_xNb_{0.1}O_{3\pm\delta}$	1173, 12 in alumina	1773, 24	ball milling, 6h, 2-propanol	cubic	
$BaCe_{0.8}Gd_{0.2}O_{3-\delta}$	1523, 15(3 times)	1873	agate mortar and 2 times attrition milling	multi-phase	[41]
$BaCe_{0.8}Gd_{0.2}O_{3-\delta}$	1473, 24	1723	*	orthorhombic	[42]
$BaCe_{0.9}Y_{0.1}O_{2.95}$	1673, 5	1573, 10	ball milling,24h, agate mortar grounding again ball milling, 24, ethanol	orthorhombic	[43]
$BaCe_{0.9}Gd_{0.1}O_{3-\alpha}$	1423, 2	1723, 3	*	orthorhombic	[44]

Table 1: The preparation conditions and basic characteristics of powders obtained from the solid-state reaction method. (* - not mentioned in the literature)

2.2 Solid-state reactive sintering method

The solid-state reactive sintering method (SSRS) consists of phase formation and sintering in a single step in contrast to the typical solid-state sintering method (SSS) which comprises the compression of previously made phase. In the SSRS process, stochiometric amounts of precursors are mixed with a sintering additive and fired in a single process. This method can decrease the total cost of production, and time of the process and provide densified material at a lower sintering temperature than the conventional way.

Gorbova *et al*., (2008) carried out a study on $BaCe_{1-x}Gd_xO_{3-\alpha}$(BCG), $BaCe_{0.99-x}Gd_xCu_{0.01}O_{3-\alpha}$ (BCG–Cu), and $BaCe_{0.9-y}Gd_{0.1}Cu_yO_{3-\alpha}$. He compared the calcination temperature of the conventional solid-state method with that of the solid-state reactive sintering method. Gadolinium doped BC was calcinated at 1673 K whereas Cu added sample was calcinated at 1423 K which gave similar results. Here Cu acts as a sintering additive which also lowers the calcination temperature by 250 K. From XRD analysis, BCG samples with *x* value between 0 and 0.2 and BCG–Cu samples with *y* value between 0.0075 and 0.07 are found to be single-phased orthorhombic perovskite structure. In wet air, the total conductivity of the BCG system has a maximum value of 68 mS cm^{-1} at 1173 K for *x*= 0.2. But in the same atmosphere, BCG – Cu conductivity reached a value of 92 mS cm^{-1} [19]. Later they studied the same with other transition metals such as Fe, Ni, and Zn as sintering additives. They obtained the same results in calcination temperature but other properties like conductivity had variations. The copper enriched sample showed the highest conductivity (87 mS cm^{-1} at 1173 K) [45].

In 2010, Tong *et al*., investigated $BaCe_{0.8}Y_{0.2}O_{3-\alpha}$ through a solid-state reactive sintering method with NiO as a sintering agent. The precursors were calcinated at a temperature between 1473 and 1723 K for 12 h. The optimized condition was 1673 K with 1.0 wt% NiO. The optimized sample got a higher relative density (>98%) and a very large grain dimension of about 10 µm with the second phase of BaY_2NiO_5. Whole conductivity of 2.7 (wet Ar) and 5.9 mS cm^{-1} (wet 5% H_2 + 95% Ar) obtained for NiO-modified BCY20 samples [46].

2.3 Wet chemical methods

To solve problems arising in the solid-state reaction method, wet chemical methods such as coprecipitation, combustion (sol-gel method, Pechini method), etc. are used. The

compound synthesized from these methods has several significant advantages - finer particle size, high homogeneous crystal formation, highly purified product, and lower calcination temperature [6].

2.3.1 Co-precipitation method

The co-precipitation method is a wet chemical method used to prepare multielement oxide ceramics through the production of an intermediate precipitate to confirm the chemical consistency of ceramics, following calcination. It involves precipitating the metals in the form of hydroxide from salt precursors with the addition of a base in a solvent. Nano dimension ceramics have been prepared by researchers under controlled circumstances using this method [14]. The co-precipitation method contains certain steps including a) mixing of stoichiometric reactant nitrates in deionized water, b) addition of precipitation agent into the mixture, c) adjusting *pH* of the solution to complete the precipitation and d) adequate washing, drying, and calcination [6].

Flint *et al*., (1995) prepared $BaCe_{1-x}Ca_xO_{3-\alpha}$ and $BaCe_{1-x}Gd_xO_{3-\alpha}$ using barium nitrate, acidified cerium nitrate, and calcium nitrate or gadolinium acetate mixed in deionized water. For instant oxalate coprecipitation, aqueous ammonium oxalate was added. The mixture was centrifuged and washed with water, again centrifuged 3 times, and dried at 393 K overnight. At last, calcined it which yields crystals of orthorhombic structure. Single-phase perovskite is attained after calcination in the air for 10 h at 1273 K which is some hundred degrees lesser than the temperature (1523 K) needed to calcinate the solid oxide-carbonate mixture [47]. Meng *et al*., (2000) synthesized $BaCe_{0.9}Nd_{0.1}O_{3-\alpha}$ using the same procedure and prepared a thick membrane using the screen-printing method. The membrane obtained here was a gas-tight and crack-free dense membrane of thickness less than 10 µm. The activation energy for conduction was in the range of 0.415 eV (Ar atmosphere), which is much less than that of bulk material [48].

Zolkos *et al*., (2005) prepared Nd and Mn-doped BC perovskite and investigated the effect of *pH*, surfactants, and calcination temperature on the final product. They also synthesized the sample using ammonium carbonate in place of ammonium oxalate and found similar properties in the formation of the perovskite. They varied the *pH* of the initial solution to study its effect on the particle dimension. For low *pH* values, CeO_2 impurity was found and perovskite had a large plate-like shape. At about 8 *pH* value, pure perovskite particles formed without any other crystal phases, and the particles had a round shape of 100 to 200 nm in size.

They concluded that, in coprecipitation synthesis, a neutral *pH* value is needed for pure crystal phase production. With the use of surfactants, no noteworthy decrease in the particle dimension of perovskites was detected [14].

Kim-Lohsoontorn *et al*., (2015) made a novel combustion method using ultrasonic-assisted precipitation along with conventional precipitation methods with different precipitation agents (ammonium oxalate and sodium hydroxide) to prepare BC. For the ultrasonic-assisted precipitation method, the consequence of ultrasonic intensity was investigated. For the low-intensity experiment, the solution in the beaker was placed on an ultrasonic bath of an intensity of 30 W cm^{-2}. For high intensity, a high-intensity ultrasonic prob (150 W cm^{-2}) was immersed in the solution. The materials were collected as precipitated and calcinated at 1173 K for 5 h. From their investigation, they concluded that precipitation parameters such as precursors, precipitation agent used, the concentration of precipitation agent, and temperature have a significant effect on the crystallite size, phase formation, and percentage of perovskite formed. Preparation using ammonium oxalate provided single-phase BC perovskite and sodium hydroxide provided a mixture of BC and ceric oxide phases. The percentage of perovskite formation and the crystallite dimension of the product increased with an increase in temperature and concentration of precipitation agent. The usage of ultrasonic during preparation helped in the formation of uniform particle dimensions and shape dispersal. The percentage of perovskite formation also increased with ultrasonic use due to improved kinetics as a result of turbulent flow and shock waves formed by consistent cavitation. A summarization of the conditions and characteristics of the products is shown in the table 2 [49].

Method		precursor used	precipitation aid	concentration of precipitation(M)	temperature (K)	% perovskite		Crystallite size (nm)	
conventional method		chloride base	sodium hydroxide	20	298	26.6	50.6	6.4	23.9
				20	343	26.7	52.8	7.6	28.7
				20	363	31.9	62.5	8.2	34.2
				15	363	29.1	37.4	7.7	23.7
				10	363	28.8	37.3	7.1	20.9
		nitrate base	ammonium oxalate	1	363	30.6	100	18.7	29.8
ultrasonic assisted	low intensity	chloride base	sodium hydroxide	20	363	23.5	65.7	4.9	27.1
		nitrate base	ammonium oxalate	1	363	17.9	100	7.6	27.5
	high intensity	chloride base	sodium hydroxide	20	363	49.6	74.9	4.2	15.2

		nitrate base	ammonium oxalate	1	363	45.9	100	6.3	18.4

Table 2: Different parameters of product synthesized using conventional and ultrasonic-assisted precipitation methods [49].

In 2017, Verbova *et al*., synthesized undoped BC using the conventional co-precipitation method with ammonium oxalate as a precipitant and studied the effect of calcination in vacuum and air separately. They found out that calcination in vacuum leads to the formation of BC perovskite with a reduced size of the coherent region of crystallite at a lower temperature (at 1123 K) compared to calcination in air. From the SEM image, the average particle dimension is about 10 μm and the prepared sample was very fine which spread all over the sample [50, 51]. The preparation conditions and basic characteristics of powders obtained from the co-precipitation method is illustrated in table 3.

Material	precursors	coprecipitant	calcination temperature(K), time (h)	precipitation temperature(K)	structure	reference
$BaCeO_3$	nitrates	diammonium oxalate monohydrate	1373, 2 in air or 1273, 4 in vacuum	353	*	[9]
$BaCe_{0.7}Zr_{0.1}Y_{0.2}O_3$	nitrates	ammonium carbonate	1373, 3	*	*	[6]
$BaCe_{0.9}Nd_{0.1}O_{3-\alpha}$	nitrates	ammonium oxalate	1373	373	*	[12]
$BaCe_{1-x}Ca_xO_{3-\alpha}$	nitrates	ammonium oxalate	1523, 10	393	orthorhombic	[47]
$BaCe_{1-x}Gd_xO_{3-\alpha}$	Ba and Ce nitrates and Gd acetate	ammonium oxalate	1523, 10	393	cubic	
$BaCeO_3$	nitrates	ammonium acetate	1173, 5	363	orthorhombic	[49]
$BaCeO_3$	nitrates	ammonium oxalate	298 -1223 both in air and in vacuum	353	*	[50, 51]
$BaCeO_3$: Gd	Ba, Ce nitrates, and Gd oxide	ammonium hydroxide	873, 4	363	orthorhombic	[52, 53]
$BaCe_{0.7-x}Sm_xZr_{0.2}Y_{0.1}O_{3-\alpha}$	nitrates	sodium carbonate	1473, 4	363	cubic	[54]
$BaCeO_3$ and $BaCeO_3$: Nd	nitrates	ammonium hydroxide	1373, 12	*	orthorhombic	[55]

Table 3: The preparation conditions and basic characteristics of powders obtained from the co-precipitation method (* - not mentioned in the literature).

2.3.2 Combustion synthesis

The combustion method of preparation is an easy and appropriate way for the production of a wide variety of advanced perovskite materials. This method is based on the thermally tempted oxidation-reduction reaction between the fuel and oxidant. Many different types of combustion techniques are there which differ in combustion mode or reactants' physical state. For the preparation of monophase nanopowder, it is considered one of the best methods with uniform microstructure, shorter reaction time, and lower working temperature compared with other conventional routes [8].

Khani *et al.*, (2010) prepared nanoparticle core-shell electrolyte materials for proton ceramic fuel cells using yttrium-doped barium zirconate as the core and yttrium-doped barium cerate as the shell. They synthesized $BaCe_{0.8}Zr_{0.1}Y_{0.1}O_{2.95}$ (BCZY10) by using an appropriate amount of constituent acrylates formed from their acetate salts which were mixed independently in an aqueous mixture of acrylic acid and ammonium hydroxide. Each solution was refluxed overnight and condensed independently using rotary evaporation. The resulted mixtures were mixed and again refluxed. To remove the solvent, the solution was rotary evaporated and a gel form was obtained. To get solid BCZY10, the viscous gel was calcinated at 673 K for 3 h and annealed at 1173 K for 4 h. BCY10 was also prepared using the same technique. The resulted conductivity in moist N_2 atmosphere of BCY10 synthesized by this method (2×10^{-2} S cm^{-1} at 873 K) is equal to or greater than that reported for samples of similar composition synthesized by direct ceramic solid-state preparation methods [3]. Greater CO_2 uptake was obtained for BCY10 (13%) powder than for BCZY10 powder (10%) which is in agreement with the literature report that partial incorporation of Zr in place of Ce increases chemical stability in BCY10 [3, 56].

Tb-doped BC of different compositions was prepared by Islam *et al.*, (2013) using glycine as fuel. In this investigation, apart from barium excess or stoichiometric composition, barium deficient composition was chosen for better chemical stability along with nitrate–fuel ratio of 0.17. The synthesized powder was calcinated at 1373 K for 6 h which is observed as the minimum temperature for perovskite phase formation which was obtained from TGA. From TGA, major weight loss for all compositions occurred between 473 – 698 K which indicates gradual decomposition. They found that electrical conductivity rises with upward Tb concentration both in a moist atmosphere and in air and also with temperature [57].

Medvedev *et al*., (2013) investigated the effect of different fuels such as glycerin, glycine, and citric acid in the synthesis of the material (1-x) $Ce_{0.8}Sm_{0.2}O_{2-\alpha}$ - $xBaCe_{0.8}Sm_{0.2}O_{3-\alpha}$. To remove undecomposed particles and nitrates and to get desired oxide particles, the powders were heated at 873 K for 5 h and the synthesis was done at 1373 K for 3 h. The great porous structure of the powders is the consequence of the huge amount of gases released during combustion. The crystallite dimension and sample morphology depend on the kind of fuel used. The crystallite dimension tends to reduce with adiabatic temperature and reaction enthalpy. Using a mixture of ethylene glycol, glycerol, and citric acid leads to vigorous foaming of the resultant compound before combustion and further production of finely distributed powder. Whereas the usage of citric acid and glycine causes violent combustion of the nitrate–fuel mixture and production of partially sintered powder. There was no change in the mass of powder on heating from 1353 K for all the combinations which indicate the complete perovskite formation. $BaCe_{0.8}Sm_{0.2}O_{3-\delta}$ sample prepared with glycerol has an orthorhombic structure. The finest powder was formed when glycerol was used [58, 59]. The preparation conditions and basic characteristics of powders obtained from the combustion method is illustrated in table 4.

Citrate-nitrate auto combustion method (CNA)

The citrate-nitrate auto-combustion method is a common solution combustion synthesis in which metal nitrates and citric acid as fuel are taken as precursors. This method can be more appropriately labeled as the sol-gel combustion method and shows certain similarities with the Pechini method. The major difference between CNA and Pechini methods is that the nitrates are not removed as NO_x, but persist in the solution to cause auto combustion [8]. This method provides the highest homogeneity and simple mixing of the reactants without additional grinding or additional mixing steps with various thermal treatments [1].

Accardo *et al*., (2020) investigated the influence of cobalt addition on different properties of $BaCe_{0.85}Gd_{0.15}O_{3-\delta}$ using the sol-gel combustion technique. BC codoped with gadolinium and cobalt electrolyte powders were synthesized from corresponding nitrate precursors. Citric acid was added into an aqueous solution of nitrate precursors with 1: 1 molar ratio and heated for 30 min at 353 K to get a viscous gel. To initiate combustion, the temperature was changed to 523 K. After the synthesis, the sample was calcinated for 2 h at 1473 K to remove impurities. Raman and XRD revealed that doping of cobalt element stabilized perovskite arrangement which favors a greater symmetry structure because of the

substitution of cobalt in the Ce site rather than the Ba site [1]. The materials $BaCe_{0.8-x}Zr_xY_{0.2}O_{3-\alpha}$ were synthesized by Lyagaeva *et al*., (2015) with the addition of sintering aid CuO (1723 K / 4h). The addition of a sintering aid allowed to synthesis dense samples and to study the thermal expansion more clearly. From XRD analysis, the sintered sample is single-phase over the whole range of zirconium concentrations. The perovskite has an orthorhombic shape for x = 0.1, 0.2, and rhombohedral or cubic for $x \geq 0.4$. Symmetry increases with the value of x which is confirmed by making the Goldschmidt tolerance factor one [60].

Deganello *et al*., (2009) made a dense investigation on the CNA method by varying the fuel- oxidant stoichiometric ratio (F/O), *pH* value, and citric acid-metal nitrate ratio(C/M) and prepared the material $BaCe_{0.9}Y_{0.1}O_{3-\alpha}$ along with other perovskite nanomaterials. The flame combustion proceeds until the F/O ratio reached 0.4. No segregation was found for the high F/O ratio. Orthorhombic perovskite-type key phase cell parameters remain persistent for a high F/O ratio up to 0.8. The particle dimension at a low F/O ratio is about 200 nm which increases further, but the crystallite dimension keeps on constant at 120 nm and the surface range is lesser than 5 $m^2\ g^{-1}$ and persistent with the F/O ratio. A small *pH* value harms resultant morphology and a large *pH* value may produce segregation of dopants. So, a *pH* value of about 4 is considered a good choice. A low value of the C/M ratio influences the morphology and a high value of the C/M ratio adversely affects the phase composition and perovskite formation temperature. So, a C/M ratio of about 2 is considered a good choice [8].

Acetate – H_2O_2 combustion method

The acetate-H_2O_2 combustion method was developed by Nasani *et al*., (2013) which is an economical, modest and eco-friendly preparation method, and avoids the emission of NO_x gases which is the typical by-product of nitrate precursor methods. They prepared $BaCe_{0.8-x}Zr_xY_{0.2}O_{3-\alpha}$ using barium, cerium, zirconium, and yttrium acetates with 30 wt% hydrogen peroxide. Hydrogen peroxide has a dual role here both as an oxidation agent and in the creation of peroxide metal complexes. This novel combustion method resulted in powder with a crystallite size of 10 – 20 nm as prepared and 30- 60 nm as calcinated (1373 K or 1623 K for 6 h). A pure perovskite phase was formed after calcination at 1623 K. The proton conductive behavior of the sample was studied by using AC impedance spectroscopy in a wet N_2 atmosphere and was similar to literature behavior. In this work, they highlighted the efficiency of this novel method in the synthesis of stoichiometrically accurate barium cerate [61].

Composition	materials used	calcination temperature (K) and time(h)	structure	Fuel, fuel to oxidant molar ratio (F/O)	reference
$BaCeO_3$	nitrates	773-1273, 4	rhombic	Hydrazine, 1.2	[2]
$BaCe_{0.8}Zr_{0.1}Y_{0.1}O_{2.95}$	acrylates	1173, 4	*	acrylic acid and NH_4OH	[3]
$BaCe_{0.9}Y_{0.1}O_{3-\alpha}$	acrylates	1173, 4	orthorhombic	acrylic acid and NH_4OH	[3]
$BaCe_{0.9}Y_{0.1}O_{3-\alpha}$	nitrates	1273, 5	orthorhombic	citric acid, 0.4-1.6	[8]
$Ba_{0.8}Ce_{1-x}Tb_xO_{3-\alpha}$	nitrates	1373, 6	orthorhombic	glycine	[57]
(1-x) $Ce_{0.8}Sm_{0.2}O_{2-\alpha}$ - x$BaCe_{0.8}Sm_{0.2}O_{3-\alpha}$.	nitrates	873, 5 then 1373, 3	*	glycine, glycerol, or citric acid and with a combination	[58]
$BaCe_{0.8}Sm_{0.2}O_{3-\alpha}$	nitrates	1373, 3	orthorhombic	glycerol	[58]
$BaCe_{0.8-x}Zr_xY_{0.2}O_{3-\alpha}$	corresponding Nitrates and CuO or Co_3O_4	1423, 5	Orthorhombic (x=0, 0.1, 0.2)	citric acid	[60]
$BaCe_{0.8}Y_{0.1}Zr_{0.1}O_{3-\alpha}$	$Ce(NO_3)_3.6H_2O$, $Y(NO_3)_3.6H_2O$, $ZrOCl_2.8H_2O$, $BaCO_3$	773, 4	Single phase	citric acid and ethylene glycol	[62]
$BaCeO_3$: Eu	cerium and barium nitrates, europium oxide	1273-1573, 5	orthorhombic	urea	[63]
$BaCeO_3$: Y	nitrates	1273, 5	orthorhombic	citric acid and ammonium nitrate, 0.4	[64]
$BaCe_{1-x}Y_xO_{3-\alpha}$	nitrates	1273, 5	Single phase	citric acid, ammonium nitrates, and ammonium hydroxide, 0.4	[65]
$BaCe_{0.9}Sm_{0.1}O_{3-\alpha}$	nitrates	1273, 4	orthorhombic	citric acid, 2:1	[66]
$BaCe_{0.5}Zr_{0.35}Y_{0.15}O_{3-\alpha}$	nitrates	1473, 2	*	citric acid	[67]
$BaCeO_3$	nitrates	1423	orthorhombic	citric acid and ethylene glycol	[68]

Table 4: The preparation conditions and basic characteristics of powders obtained from the combustion method (* - not mentioned in the literature)

2.3.3 Sol-gel method

Li *et al*., (2007) prepared $BaCe_{0.9}Sm_{0.1}O_{3-\delta}$ and $BaCe_{0.8}Gd_{0.1}Sm_{0.1}O_{3-\delta}$ using the sol-gel method. Barium nitrate and ammonium cerium nitrate were added to the nitric acid solution of samarium oxide. Solid citric acid was then added to it to get 1:1 C/M molar ratio. The mixture was then placed in a water bath at 333 K for evaporation up to the formation of a viscous liquid. The temperature was then changed to 373 K for 5 h to form a gel-like porous mass. After placing the gel in a dry oven for 5 h at 383 K, it changed into a solid mass. This was crushed using an agate mortar and calcined for 5 h at 973 K. A powder was obtained with ultrafine morphology for both $BaCe_{0.9}Sm_{0.1}O_{3-\delta}$ and $BaCe_{0.8}Gd_{0.1}Sm_{0.1}O_{3-\delta}$. This procedure seems to be very time-consuming, but the obtained material had most of the features as expected. From TG and DTA analysis, the optimum temperature of calcination was found to be 923 K for $BaCe_{0.9}Sm_{0.1}O_{3-\delta}$ and 953 K for $BaCe_{0.8}Gd_{0.1}Sm_{0.1}O_{3-\delta}$. XRD analysis exposed a single

perovskite structure with few impurities. SEM analysis was done to examine microstructure and found distinct grains having wide distributed sizes and high porosity [69].

Osman *et al*., (2008) prepared $BaCe_{0.95}Yb_{0.05}O_{2.975}$ using cerium acetate hydrate, barium acetate, and ytterbium acetate hydrate as starting materials. A calcination temperature of 1273 K for 5 h produced a sample with a homogeneous, single-phase structure and reduced particle size. The sample shows more dc conductivity at a raised temperature and the conduction was governed by electronic or oxide ions in a water vapor atmosphere. While it exhibited lower mechanical stability after keeping it in a desiccator for 2 months and in a CO_2 atmosphere, showed poor chemical stability [70].

Modified sol-gel method

The modified sol-gel process is a polymerized complex method for synthesizing ultrafine powder morphologies with greater phase purity. In the preparation of $BaCe_{0.54}Zr_{0.36}Y_{0.1}O_{2.95}$ role of a combination between ethylenediamine tetraacetic acid (EDTA) and citric acid (CA) as chelating agents was thoroughly investigated by Abdulla *et al*., (2013). They prepared the material using three different processes named as CA method, EDTA method, and CA–EDTA method. For the CA process, a distilled water solution of nitrates of reactants was stirred continuously in a magnetic stirrer. Citric acid was slowly added to the mixture to form a citric acid-metal complex. In the EDTA process, an ammonia solution of 25 % was added (to facilitate dissolution of EDTA in water) to a mixture of EDTA and deionized water at a *pH* value of 6. This solution was added to metal nitrate solution in deionized water under magnetic stirring to form a metal – EDTA complex maintaining a *pH* of 6. In the CA-EDTA process, ammonia solution was added to the mixture of EDTA and deionized water to form EDTA solution. This EDTA solution was added to the metal nitrate solution following the addition of the desired amount of citric acid (metal: CA: EDTA = 2:1:1) to form CA -EDTA metal complex. The resulting solutions from the three routes were named S1, S2, and S3 respectively. Ethylene glycol and ammonia solution were added to maintain a *pH* of 6-7 under stirring. The resulting solution was heated and stirred at 363 K to get a dark brown gel. This gel was dried overnight on a hot plate and calcinated at 598 K, 823 K and 1373 K for 10 h to get desired material. From TGA results, it was found that thermal decomposition of the CA-EDTA sample, S3 (1023 K) is lower compared to S2 (1043 K) and S1 (1073 K). Due to the insufficiency of citric acid for chelating all metal ions, the heat released for S1 is greater. It was found that the combination of CA–EDTA method act as a better method to impact thermal

decomposition performance and increase production rate compared to the separate citric acid and EDTA method. Different Chelating agents have different electron-donating groups, which influenced BCZY's thermal behavior. FTIR and TGA results showed that a temperature greater than 1373 K is required to decompose the remaining carbonates [71].

2.3.4 Pechini process

The Pechini method is one of the liquid phase reaction methods used to prepare perovskite oxide nanopowders. It is an improved version of the nitrate combustion process and sol-gel method. The primary difference is as follows: in the case of the Pechini process, the fuel or combination of fuels is put into the mixture of metal nitrates in a fraction exceeding the stoichiometric amount which results in the creation of the gel-like product during water evaporation. To decompose and remove gas constituents, further annealing at 473 K to 773 K is needed. This product is having high dispersion and can be sintered to high perovskite ceramics at minimal temperature. Fuels like citric acid, EDTA, and ethylene glycol, and their combinations are commonly used reducing agents in the case of BC-derived perovskites [72].

Agrawal *et al*., (1997) synthesized $BaCe_{0.8}Gd_{0.2}O_{3-\delta}$ thin films with ethylene glycol and EDTA as a chelating agent. Here EDTA improved the homogeneity of distribution of metal ions in the solution. To enhance the dissolution of EDTA in demineralized water, ammonium hydroxide was used. The variables studied here are EDTA/EG ratio, BCG sol viscosity, and C ratio (the molar ratio of chelating agent to metal ions). EDTA/EG ratio varied from 1 to 0.17 and didn't have much effect on the BCG sols. Viscosity higher than 0.0025 Pa.s was required for suitable wettability of BCG sols and lesser than 0.0025 Pa.s caused poor wettability. Viscosity higher than 0.005 Pa.s resulted in the precipitation in the solution. The most crucial parameter in this process is the C ratio. The homogeneous and crack-free film was obtained at an intermediate C ratio (2.5>C>1.5). Hence optimization of the C ratio and viscosity is needed in the sol to get sol without precipitate. From the XRD pattern, they concluded that the modified Pechini process resulted in a significant reduction in the processing temperature (1023 K) of BCG films [73]. Khandelwal *et al*., (2011) used additional milling processes to reduce particle size in the preparation of perovskite. From the analysis of particle size, it was found that particle size decreased to half its initial value after ball milling [74].

Sergiienko *et al*., (2017) prepared $BaCe_{0.7}Y_{0.2}In_{0.1}O_{3-\delta}$ by modified Pechini method following decomposition of the organometallic blend at elevated temperature. Citric acid and glycerol were used as the chelation agent with the addition of ammonium nitrate to enable

proper dissolution. They prepared samples of different conditions with the molar ratio as Ba: Me: glycerol: citric acid: ammonium nitrate = 1: 1: 30: 10: 10 and samples of a slight amount of additional barium (Ba: Me: glycerol: citric acid: ammonium nitrate = 1.02: 1: 30: 10: 10). Here calcination was carried out for 6 h at 1303 K and 1523 K in the air to prepare different samples. The grain size of the sample prepared at 1303 K was about 0.1 to 0.2 µm and that of 1523 K was agglomerates of micron size. Calcination at 1523 K caused decomposition of residual $BaCO_3$ and evaporation of other impurities which resulted in extra shrinkage of the powder [7].

Later Deng *et al.*, (2019) investigated thoroughly the Pechini method to prepare BC perovskites. They determined optimum experimental parameters such as water bath temperature, metal ion concentration, and dosage of ethylene glycol and citric acid for the pure homogeneous phase formation. The optimal experimental conditions for preparing single-phase BC nanopowders were determined: 343 K gelation temperature, 0.05 mol L^{-1} of total metal ion concentration, 1:5 total metal to citric acid molar concentration ratio, and 2:1 molar ratio of ethylene glycol to citric acid and 1173 K calcination temperature for 4 h [75].

Material	polymerization/ complexation agent	calcination temperature/ time (K/h)	grain size	Complexation agent to metal ion ratio	reference
$BaCe_{0.7}Y_{0.2}In_{0.1}O_{3-\delta}$	citric acid, glycerol and ammonium nitrate	1343/ 6	0.1 to 0.2 µm	5:1	[7]
$BaCe_{0.7}Y_{0.2}In_{0.1}O_{3-\delta}$ with excess barium	citric acid, glycerol, and ammonium nitrate	1523/ 6	Micron size	5:1	[7]
$BaCeO_3$: Gd	citric acid and ethylene glycol	1173/ 4	6.77 µm	5:1	[53]
$BaCe_{0.8}Gd_{0.2}O_3$	EDTA, ethylene glycol and ammonium hydroxide	1023	Sub micron	2.5 to 1.5 :1	[73]
$BaCeO_3$	citric acid and ethylene glycol	1173/4	50 nm	5:1	[75]
$BaCe_{0.8}Y_xNd_{0.2-x}O_{3-\delta}$	citric acid and EDTA	773/2	10-20 nm	2:1	[76]
$BaCe_{0.8}Gd_{0.2}O_3$	EDTA, EG and ammonia	1273/ 4	*	1.5:1	[77]

Table 5: The preparation conditions and basic characteristics of powders obtained from the Pechini method(* - not mentioned in the literature)

2.3.5 Growth of barium cerate crystal from $BaCl_2$ solution

1.5 mm sized BC crystals were prepared from a molten solution comprising barium oxide, cerium oxide, and barium chloride. Barium chloride was used as a flux. Due to the lower

solubility of cerium oxide in the molten barium chloride, the maximum dimension of the crystal is restricted. The flux, barium chloride separated by the discharge of the molten material with water. Preparation composition, conditions, and results are given in the following table [4].

Sl No	starting composition	soaking time (h)	maximum temperature after soaking (K)	cooling rate	crystal products
1	a. 21 g of $BaCl_2$. $2H_2O$ b. 5.46 g of $BaCO_3$ c. 4.76 g of CeO_2.	2	1433	2K h^{-1} up to 1173 K	Sandy and small transparent crystals of max. dimension 0.5 mm.
2	a. 21 g of $BaCl_2$. $2H_2O$ b. 5.46 g of $BaCO_3$ c. 4.76 g of CeO_2.	12	1473	4K min^{-1} to 1073 K	
3	a. 24.43 g of $BaCl_2$. $2H_2O$ b. 6.95 g of $BaCO_3$ c. 3.6 g of CeO_2 (seeds were used)	2	1523	0.625K min^{-1} to 1373 K	Dark brown crystals of max. dimension 1.5 mm
4	a. 24.43 g of $BaCl_2$. $2H_2O$ b. 6.95 g of $BaCO_3$ c. 3.6 g of CeO_2.	2	1573	0.625 K min^{-1} to 1423 K	White crystals of max. dimension 0.8 mm

Table 6: preparation compositions and conditions of growth of BC crystals from $BaCl_2$ solution.

From thermal analysis, it was found that barium chloride loses its complete crystal water under flowing air in 353-453 K temperature range. After dry mixing, the mixture was transferred into an alumina crucible covered with a lid to prevent loss of flux through evaporation. In some experiments, seeds of BC from the former experiment were held in the center of the molten material by using a platinum spoon. And also, the temperature of growth should be minimum to prevent evaporation. Because of the stability of the crystals formed in this way in the water, cold water leaching was used to remove the solvent. These crystals are fairly not stable in dilute acids. Barium chloride was found to be a hopeful candidate for the preparation of BC crystals. But cerate is less soluble in barium chloride which is the limiting factor of this method [4].

2.3.6 Microemulsion reaction method

Zolkos *et al*., (2005) prepared BC using nitrates of barium and cerium. Nitrates of barium and cerium and ammonium carbonate or ammonium oxalate were dissolved in demineralized water separately. By mixing cyclohexane, 2 – methyl -1- propanol, and surfactants such as Triton X – 114, tergitol NP – 7, or triton X – 100, an organic phase was made and was separated into two. As prepared two aqueous solutions were mixed in these two

mixtures and stirred well. They were mixed to get barium–cerium oxalate or carbonate in nanosized aqueous droplets after the formation of the microemulsion solution. The size of the particle of the precipitate was restricted by the aqueous droplet size. The precipitate formed was then filtered using acetone for removing surfactants and dried by freezing. Obtained powders were then calcined at 773 K in the air for removing residual surfactants and organic solvents. It had a particle size of 5 – 10 nm. The product thus obtained was then reheated at 1173 K to get a perovskite structure of 40 nm size. The particles thus obtained were mostly round, minimal, and least agglomeration [14]. Khani *et al*., (2009) investigated $BaCe_{0.9}Y_{0.1}O_{3-\delta}$ using the same procedure with n-octane as an emulsifier and 1 butanol and Brij 56 as surfactants. From High-resolution microscopy, 25 to 35 nm-sized particles were found [78].

2.3.7 The molten salt reaction method

In the molten salt reaction method, cerium and barium salts were added to various molten salts to form perovskites. Zolkos *et al*., (2005) synthesized BC using molten salt of NaOH/KOH, KNO_3/$NaNO_3$, and KCl /LiCl eutectic mixture. Different salts of barium and cerium such as oxalate, nitrates, and hydroxide were introduced into the molten salts at various temperatures (673 K, 773 K, 873 K, 973 K, 1073 K, and 1173 K) for 5 h to investigate the formation of BC in these molten salts. From XRD analysis, it has been found that the products had only cerium oxide and barium salts for all the molten salts used. So, they performed a thermal stability experiment with BC dissolved in molten salts and showed that it is unstable in molten salts [14].

In contradiction, later Gdula-Kasica *et al*., (2012) successfully synthesized $BaCe_{0.8}Y_{0.1}Zr_{0.1}O_{3-\alpha}$ using the molten salt method. The precursors used were barium nitrate, oxides of yttrium, cerium, and zirconium with excess barium nitrate to reimburse evaporation of barium. Using the combination of KCl and NaCl, the precursors were ball milled in a 1:2 salt to precursor molar ratio. Then the mixture was calcinated at 1263 K for 2 h in air. The salt was removed by frequent washing with deionized and acidified water of pH 5. After drying the precipitate, it resulted in a yellowish homogeneous powder of the desired composition of 50 nm crystallite size. These crystallites often agglomerated into huge grains and a little cerium oxide and barium carbonate were spotted from XRD [62].

2.3.8 Hydrothermal synthesis using HMTA

Bhowmick *et al*., (2010) prepared BC nanoparticles by hydrothermal synthesis using hexamethylenetetramine (HMTA). Here HMTA supplies hydroxyl ions to initiate the

precipitation reaction in the mixture. In this method 0.012 mol L^{-1} aqueous solution of barium nitrate, cerium nitrate, and HMTA were prepared separately. These solutions were mixed and put in a water bath at 353 K of ambient pressure. 40 – 60 minutes later the solution's color changed into milky which is an indication of the formation of the nanoparticle. To get dry powder, it was then heated at 423 K on a hotplate to eliminate water. The obtained powder was then annealed at different temperatures (873 K, 973 K, 1073 K) for 10 h. after the synthesis process at 353 K, particles exhibited cubic morphology and converted into mixed multi-faceted and equiaxed morphology as calcinating temperature increased to 1073 K. At the edges of the nanoparticle, surface steps were crystallographically oriented. In some nanoparticles, microstructural features including small-angle grain boundaries and edge dislocation are observed [79].

2.3.9 Cryogenic method

Amsif *et al*., (2009) synthesized $BaCeO_3$ and $BaCe_{0.9}Y_{0.1}O_{3-\delta}$ using the cryogenic method from the nitrate precursors dissolved in deionized water. EDTA was used as the complexing agent and to fix *pH* value at 7 to 8, ammonium hydroxide was used. The resulting solution was then dropped into liquid nitrogen. When the nitrogen was completely evaporated, the obtained solid residue was lyophilized, calcinated at 573 K for dehydration, and annealed at varying temperatures (1073– 1273 K). Single-phase perovskite was obtained only after calcination at 1273 K temperature. Samples of $BaCe_{0.9}Y_{0.1}O_{3-\delta}$ sintered for 4 h at 1773 K and had 99% relative density with the narrow spreading of grain size (2.5 μm average grain size) [80]. Later they synthesized $BaCe_{0.9}Ln_{0.1}O_{3-\delta}$ (Ln=Nd, La, Gd, Sm, Y, Yb, Tb) powders by a similar technique. The relative density of samples sintered for 4 h at 1673 K had a 96% relative density for Ln = Yb, Sm, Nd, Gd and 91–95% for Ln =Tb, La, Y. All the samples had a grain size ranging from 1 μm to 2 μm [81].

3. Comparative study

Acceptor-doped BC compounds have dominated the research field of high-temperature proton conductors. Although they have great conductivities, they are chemically unstable in CO_2 and H_2O-containing atmospheres. Doping and codoping with other elements enhance stability. Several synthesis methods were adopted in literature works to prepare BC perovskites. Synthesis methods have also influenced the structural, physical, and chemical properties. Lots of work were done to find out which synthesis method is the best one to produce BC crystal structure.

The temperature of calcination and size of the particle in BC perovskites changed significantly with various synthesis methods. In the solid-state method, barium carbonate, cerium oxide, and dopants are usually of micrometer size with some agglomerates. Even though grinding helps in breaking the agglomerates into small particles and disperses various components in the mixture, it needs a lot of time and effort. But the perovskite formation still needs diffusion of various cations through large particles to produce a homogeneous phase, a temperature-dependent process. A temperature of about 1373 K was required to complete the diffusion and perovskite phase formation [14]. Sergiienko *et al*., (2017) made a detailed analysis of the temperature of the synthesis of yttrium-doped BC. Yttrium shows poor solubility at a temperature below 1723 K, a rise in temperature of calcination in solid-state reaction up to 1948 K for 12 h helped the formation of single perovskite phase structure even for yttrium up to 30 mol % [82], 1923 K for 4 h or 10 h [83] and 1773 K for 10 h [7, 84].

In contrast, in microemulsion and coprecipitation preparation methods, all the precursors are uniformly mixed in an aqueous solution on an atomic scale and precipitated before calcination. Only thermal decomposition of precursors is needed for the creation of perovskites and the temperature of calcination is consequently reduced to 1173 K. The calcination temperature reduction not only saves the energy in the procedure but also contributes to the synthesis of sub-micrometer and nanoparticles compared with micrometer-sized particles using the solid-state method [14].

In the coprecipitation method, the *pH* of the reactant solution is the major factor in determining the size of particles and the extent of agglomeration of perovskites. Barium and cerium cations are easily precipitated by carbonate or oxalate anions and are mixed homogeneously with each other in a neutral solution. Precipitated particles absorb extra anions onto their surface and convert them into negatively charged which prevents the aggregation of precipitated particles with each other. If the solution is made to be more acidic, it makes the precipitate to be more soluble and the absorbed anions on the particle surface become neutralized on an increase in the number of protons. In acidic solutions, higher precipitation activities, more dynamic solutions, and less absorbance on the surface of particles resulted in the aggregation of small particles into large particles. While hydroxide ions also cover the surface of particles in basic solution. These hydroxide ions on the surface may form an agglomeration of some individual particles of 200 nm size or above after calcination [14].

In the microemulsion preparation method, nanosized droplets of water in the oil phase ensure the uniform mixing of all particles in the solution while limiting coprecipitate particle dimensions. Water was removed by freeze-drying precipitates by sublimation to reduce the formation of agglomerates. All these processes have favored the creation of 5-10 nm particle-size material before calcination. In calcination, both perovskite formation and growth of particle size are occurring. During this process, decomposition of precipitates and aggregation of particles of 40 – 60 nm grain size will take place. These particles still have nano-size and decreased agglomerate strength due to the elimination of water molecules before calcination [14].

Zolkos *et al*., (2005) compared the formation of BC membranes by different synthesis procedures. When compared with the solid-state method, the microemulsion and coprecipitation method needed a 200 K lower temperature of calcination to synthesize perovskite phase of uniform chemical composition and fewer agglomerate particles of sub-micrometer or nano size. In the microemulsion method, perovskite particles were 40 – 60 nm in size with lower agglomeration among particles. The particle size of the sample prepared from the solid-state reaction was 5-20 µm after calcination at 1573 K. Size of particles prepared from coprecipitation methods depends on the *pH* of the solution. Doping with Mn and Nd improved sinterability and resulted in a closely packed perovskite membrane after sintering. Preparation methods also affected perovskite membrane densities. Membrane densities decreased in the order of microemulsion > coprecipitation > solid-state method, in the opposite order of size of the particles. FESEM image revealed the existence of a lot of pores linked to each other in the membrane in the solid-state reaction product. FESEM image of the membrane formed from powder synthesized by the coprecipitation method showed that grains of perovskite were arranged tightly. Even though, some round-shaped grains were also presented which suggested the existence of a few voids in the membrane. From the FESEM image of the membrane formed from powder synthesized by the microemulsion method, all the grains of perovskite were arranged very tightly without any round-shaped grains. They concluded that the proton conductive BC membrane formed from material synthesized from microemulsion or coprecipitation had increased strength, density, and decreased porosity than that of the solid-state reaction method [14].

Chen *et al*., (1997) have done a study on $BaCe_{0.9}Nd_{0.1}O_{3-\alpha}$ prepared through coprecipitation by oxalate method (OP), solid-state method via ball milling (COB), and agate mortar technique (COM). Studies from XRD and DTA – TG analysis showed that calcination

of temperature at 1273 K or more produced a single perovskite phase for all the methods. Studies on the densification process at constant heating rate dilatometry showed that shrinkage performance for COB and OP were quite similar, but that for COM was significantly different. Open porosity and sintered density revealed that the temperature of calcination had a significant role in the sintering progression for all the methods. The powder samples from COB and OP had huge surface area, decent sinterability, and less particle dimension, whereas those from COM had less surface area, poor sinterability, and large particle dimension. Almost dense materials were obtained at a sintering temperature of 1673 K from OP and at a sintering temperature of 1573 K from COB. Whereas from COM, sintering at 1773 K yielded only porous microstructure. From electrical measurements done in the hydrogen atmosphere, the product from COM had the smallest conductivity, those from COB had higher conductivity than those from COM, and the product from OP had the largest conductivity. This result also showed that different sample preparation processes have played a significant role in conductivity [12]. By the sol-gel method, Osman *et al*., showed that at calcination of 1273 K, this method produced doped BC particles of 75-100 nm grain size which was lower than those from the oxalate coprecipitation method (7 µm) done by Chen *et al*., [70].

The atmosphere in which the sample is calcinated also has an influence on the calcination temperature. Verbova *et al*., studied the effect of calcination in vacuum and air for the preparation of BC using the oxalate coprecipitation method. XRD showed that calcination of the sample in vacuum leads to the formation of perovskite at lower temperatures with small size [50]. Diko *et al*., (2021) synthesized BC by oxalate co-precipitation, solid-state reaction method, and sol-gel method for YBCO bulk superconductor. They calcined the samples both in air and in vacuum and found which one is more effective in all three processes. The solid-state method produced samples with some huge agglomerate crystals and with the least efficiency compared to other methods. The sol-gel method, as well as the coprecipitation method and final calcination in vacuum, are much more efficient. The best outcome was obtained from the sol-gel process. Calcination in vacuum needed 100 K lower temperature for calcination than that in air for all the processes [9].

Preferable crystallite size (single, micro, and nano) for different applications is not clear. Reducing the grain size to nano in electrolytes is one of the leading factors which increases ionic conductivity. The grain boundary resistance increases with a decrease in grain size of ceramic, but according to [85], the nanocrystalline conductivity is greater than the microcrystalline. Also, the synthesis of nano-sized powders produces grains that have high

sintering ability [7]. BC nanopowders can be synthesized at a lower temperature (about 1073 K) by citrate process [86] or by using decomposition of oxalate reactants employing thermal process [87]. According to Sergiienko *et al*., for nanocrystalline samples prepared from the modified Pechini process, the time for sintering can be lowered from many hours to minutes, and also temperature for sintering can be reduced to 1573 – 1623 K [7].

Annealing at high temperatures has a significant role in improving the grain boundary conductivity of proton conductors. Following this, sintering at a high temperature is also required [88]. But at a temperature greater than 1773 K, barium may be lost through evaporation from the bulk region of BC by an accumulation of barium in grain boundary regions as an amorphous phase and cannot detect through normal XRD. And also, dopants like Gd, and Y may be redistributed to barium sites at high temperatures. Another feature of high-temperature annealing is that in micro crystallite samples, grain-boundary resistance may increase due to the possibility of accumulation of impurities phases of poor conduction in the grain boundary region [7].

To synthesize materials of high proton conductivity, dense structures are essential. It is known that BC materials require high temperatures for preparation because of their lower sinterability, and the addition of a sintering aid may increase density and lower sintering temperature. This method has been widely used for synthesizing ceria electrolytes with outstanding outcomes. Accardo *et al*., demonstrated that Pr, Bi, Li, and Co are the most efficient dopants which promote densification of ceria powders of nano-size at a lower temperature of sintering and improve their electrochemical properties using the sol-gel combustion process [1] [89] [90]. To enhance the density by reducing sintering temperature, sintering additives were added by some authors in the solid-state reaction method also, but they may reduce ionic conductivity [7].

To synthesize a compound material that has a part of the prevalence of both of the starting methods, Gdula-Kasica *et al*., combined molten salt synthesis and combustion method. To optimize the properties and microstructure of doped BC, the compound prepared from self-combustion and molten salt methods was mixed in various weight proportions to get composite materials. The influence of the addition of Ni on the morphology, conductivity, density, and phase purity was also investigated. The results of the study seemed to be very promising as the resultant compound meets the necessities of a characteristic proton conductor [62].

The luminescence property of phosphors also is greatly affected by different factors such as homogeneity, shape, size, etc., Therefore, synthesis methods have a great influence on the tuning efficiency of luminescence. The typical solid-state synthesis method meets elevated temperature of calcination, particles of microcrystalline size, agglomerates, and poor homogeneity [91]. So wet chemical methods are preferred because of their lower temperature for synthesis and improved homogeneity leading to the luminescence of high efficiency [63]. The preparation conditions and basic characteristics of powders obtained from different synthesis methods are illustrated in table 7 for comparison.

Compound	conductivity (mS cm^{-1}), atmosphere, temperature (K)	preparation method	lattice parameters			structure	activation energy (eV), temperature range of measurement	calcination temperature/ time (K/ h)	size	reference
			a(Å)	b(Å)	c(Å)					
$BaCe_{0.85}Gd_{0.15}O_{3-\delta}$	22.7, wet H_2, 1073	sol-gel combustion method	6.244	8.772	6.26	orthorhombic	0.75, 773-1073	1473/ 2	61.2 nm (crystallite size)	[1]
$BaCeO_3$	*	solution combustion method	6.252	8.79	6.227	rhombic	*	1273/4	37.6 nm (crystallite size)	[2]
$BaCe_{0.8}Zr_{0.1}Y_{0.1}O_{2.95}$	7.6, CO_2, 873	combustion method	8.777	6.227	6.225	orthorhombic	0.48, 573-873	1173/4	12-17 nm (grain size)	[3]
$BaCe_{0.9}Y_{0.1}O_{3-\alpha}$	18.2, CO_2, 873	combustion method	8.770	6.242	6.206	orthorhombic	*	1173/4	35 nm (grain size)	
$BaCe_{0.7}Y_{0.2}In_{0.1}O_{3-\delta}$	10, wet air, 1073	modified Pechini method	*	*	*	*	0.69, 1023-1223	1343/6	0.2-0.4 µm (grain size)	[7]
$BaCe_{0.9}Y_{0.1}O_{3-\alpha}$	*	citrate – nitrate auto combustion	8.774	6.244	6.244	orthorhombic	*	1273/5	120 nm (grain size)	[8]
$BaCe_{0.9}Nd_{0.1}O_{3-\alpha}$	*	solid-state method: ball milling	*	*	*	single phase	0.5, H_2, 1023-1373	873-1573/10	few µm (grain size)	[12]
$BaCe_{0.9}Nd_{0.1}O_{3-\alpha}$	*	solid-state method: mortar pestle route	*	*	*	single phase	0.51, H_2, 1023-1373	873-1573/10	few µm (grain size)	
$BaCe_{0.9}Nd_{0.1}O_{3-\alpha}$	*	coprecipitation	*	*	*	single phase	0.49, H_2, 1023-1373	773-1473/8	few µm (grain size)	
$BaCeO_3$	*	solid-state method	*	*	*	*	*	1573/5	5-20 µm (grain size)	[14]
$BaCeO_3$	*	microemulsion	*	*	*	*	*	1173/5	40 nm (grain size)	

$BaCeO_3$	$1.25X10^{-3}$ (electrical), H_2	solid-state method	6.236	6.217	8.778	orthorhombic	0.26, 275-633	1373/10 ,1873/5, 1723/10	*	[16]
$BaCe_{0.99}Nb_{0.01}O_3$	~ $3.75X10^{-3}$ (electrical), H_2	solid-state method	6.236	6.217	8.779	orthorhombic	0.32, 275-633	1373/10 ,1873/5, 1723/10	*	
$BaCe_{0.8-x}Sn_xYb_{0.2}O_{3-\alpha}$	~ 3, wet air, 873	solid-state method	4.302 (x=0.3)	-----	-----	cubic	~0.2, 473-1173	1273/8	~ 2 – 2.6 µm (grain size)	[17]
$BaCeO_3$: Y (x=0.10)	7, air, 873	solid-state method	4.398	-----	-----	cubic	0.52, 423-623	1673/10	*	[18]
$BaCe_{1-x}Gd_xO_{3-x/2}$ (x=0.10)	16, air, 1073	solid-state method	4.405	-----	-----	cubic	0.52, 423-623	1673/10	0.1 nm (crystallite size)	
$BaCe_{1-x}Gd_xO_{3-\alpha}$	68, wet air, 1173	solid-state method	8.77 (x=0.1)	6.221	6.244	orthorhombic	*	1673/2	2 µm (grain size)	[19, 45]
$BaCe_{0.99-x}Gd_xCu_{0.01}O_{3-\alpha}$	92, wet air, 1173	solid-state method	8.801 (x=0.1)	6.212	6.236	single phase	0.4, 873-1173	1423/2	10µm (grain size)	
$BaCe_{0.9-y}Gd_{0.1}Cu_yO_{3-\alpha}$	87, wet air, 1173	solid-state method	8.780 (y=0.07)	6.240	6.302	single phase	0.5, 873-1173	1423/2	*	[19]
$BaCe_{1-x}Zr_xO_3$	0.01, air, 873	solid-state method	6.24 (x=0)	8.78	6.22	orthorhombic	0.82, 573-873	1623/6	*	[20]
$BaCe_{0.5}$ $Nb_{0.5}$ O_3	*	solid-state method	4.293	-----	-----	cubic	*	1273-1473	*	[21]
$BaCeO_3$	*	solid-state method	8.786	6.251	6.220	orthorhombic	*	1273	*	[22, 92]
$BaCe_{1-x}M_xO_{3-x/2}$ (M=La, Nd, Ho)	~ 0.1 – 10, air, 1073	solid-state method	*	*	*	*	0.78-0.52, 673-1273	1373/4	*	[25]
$BaCe_{0.95}Y_{0.05}O_{3-\alpha}$	*	solid-state method	4.414	-----	-----	cubic	~ 0.29, wet N_2, 873-1173	1523/15	*	[27, 28]
$BaCe_{0.9}Gd_{0.1}O_{3-\alpha}$	*	solid-state method	4.422	-----	-----	cubic	~ 0.34	1523/15	*	
$BaCe_{0.9}Y_{0.1}O_{2.95}$	*	solid-state method	8.77	6.223	6.239	orthorhombic	*	1773/20	< 40 µm (grain size)	[29]
$BaCe_{0.9}Gd_{0.1}O_{2.95}$	*	solid-state method	8.773	6.222	6.244	orthorhombic	*	1373/15 and 1773/5	<40 µm (grain size)	[29]
$BaCe_{0.8}Gd_{0.15}Pr_{0.05}O_{3-\delta}$	25.8, wet H_2, 973	solid-state method	8.799	-----	-----	cubic	0.36, 723-973	1623/ 10	~ 10 µm (grain size)	[39]
$BaCe_{0.85}Sm_{0.15}O_{3-\delta}$	< 25.8, wet H_2, 973	solid-state method	8.784	-----	-----	cubic	0.42, 723-973	1623/ 10	few µm (grain size)	
$BaCe_{0.85}Eu_{0.15}O_{3-\delta}$	< 25.8, wet H_2, 973	solid-state method	8.773	-----	-----	cubic	0.37, 723-973	1623/ 10	few µm (grain size)	
$BaCe_{1-x}Nb_xO_{3-\alpha}$	*	solid-state reaction method	4.353 (x=0.1)	-----	-----	cubic	*	1173/12	*	[40]
$BaCe_{0.9-x}Zr_xNb_{0.1}O_{3\pm\delta}$	1.3, wet H_2, 773	solid-state reaction method	4.338 (x=0.1)	-----	-----	cubic	0.69-0.73, 673-973	1173/12	*	
$BaCe_{0.95}Gd_{0.05}O_{3-\delta}$	0.172, dry air, 569	solid-state reaction method	8.78	6.239	6.221	orthorhombic	0.49, 573-1073	1473/ 24	0.8 µm (grain size)	[42]

$BaCe_{0.9}Y_{0.1}O_{2.95}$	*	solid-state method	6.243	6.209	8.771	orthorhombic	*	1673/5	few nm (crystallite size)	[43]
$BaCe_{0.9}Gd_{0.1}O_{3-\alpha}$	5.27, air, 873	solid-state method	8.81	6.253	6.22	orthorhombic	0.644, 673-1073	1423/2 and 1723/3	few µm (grain size)	[44]
$BaCe_{0.9}Gd_{0.1}O_{3-\alpha}$: F	3.56, air, 873	solid-state method	8.805	6.252	6.217	orthorhombic	0.603, 673-1073	1423/2 and 1723/3	few µm (grain size)	
$BaCe_{0.9}Gd_{0.1}O_{3-\alpha}$: Cl	4.55, air, 873	solid-state method	8.809	6.219	6.270	orthorhombic	0.638, 673-1073	1423/2 and 1723/3	few µm (grain size)	
$BaCe_{0.9}Gd_{0.1}O_{3-\alpha}$: Br	5.07, air, 873	solid-state method	8.813	6.265	6.221	orthorhombic	0.699, 673-1073	1423/2 and 1723/3	few µm (grain size)	
$BaCe_{0.8}Y_{0.2}O_{3-\alpha}$	2.7, wet Ar, 773	solid-state reactive sintering method	*	*	*	rhombohedral	*	1673/ 12	1-3 µm (grain size)	[46]
$BaCe_{1-x}Ca_xO_{3-\alpha}$	1, N_2, 1023	oxalate coprecipitation	6.222 (x=0.1)	6.216	8.823	orthorhombic	0.6, 573-873	1273/10	*	[47]
$BaCe_{1-x}Gd_xO_{3-\alpha}$	*	oxalate coprecipitation	6.188 (x=0.1)	6.288	8.799	orthorhombic	*	1273/10	*	
$BaCe_{0.9}Nd_{0.1}O_3$	*	oxalate coprecipitation method	8.795	6.202	6.195	orthorhombic	0.89 at 973	1573/3	2-8 µm (grain size)	[48]
$BaCeO_3$: Gd	*	coprecipitation method	8.576	4.391	6.004	orthorhombic	*	873/4	10-15 nm (grain size)	[52]
$Ba_{0.8}Ce_{1-x}Tb_xO_{3-\alpha}$	49, 5% H_2 in Ar(wet), 1173	combustion method	*	*	*	orthorhombic	*	1373/6	1-6 µm (grain size)	[57]
$BaCe_{0.8}Sm_{0.2}O_{3-\alpha}$	*	combustion method	6.249	6.226	8.796	orthorhombic	0.61, wet air, 873-1173	1373/3	50.2 nm (crystallite)	[58]
$BaCe_{0.8-x}Zr_xY_{0.2}O_{3-\alpha}$	*	acetate-H_2O_2 combustion method	8.859 (x=0.1)	6.16	6.162	orthorhombic (x=0 and 0.1) and cubic for others	0.68, wet N_2, 373-1173	1373 or 1623/6	30-60 nm (crystallite size)	[61]
$BaCe_{0.8}Y_{0.1}Zr_{0.1}O_{3-\alpha}$	18.7, ambient air, 1073	composite of Self-combustion method and molten salt method	6.196	8.738	6.229	*	0.49, 573-1073	773/4 for CM and 1173/2 for MS	4 - 5 µm (grain size)	[62]
$BaCeO_3$: Eu	*	solution combustion method	8.776	6.236	6.215	orthorhombic	*	1473/ 5	135 nm (grain size)	[63]
$BaCe_{0.9}Sm_{0.1}O_{3-\alpha}$	3, air, 973	citric acid auto combustion method	8.768	6.215	6.214	orthorhombic	0.81, 723-1073	1273/10 and 1573/8	0.6 µm (grain size)	[66]
$BaCe_{0.85}Sm_{0.1}Fe_{0.05}O_{3-\delta}$	1, air, 973	citric acid auto combustion method	8.793	6.233	6.229	orthorhombic	0.46, 723-1073	1273/10 and 1573/8	1µm (grain size)	
$BaCe_{0.85}Sm_{0.1}Co_{0.05}O_{3-\delta}$	6, air, 973	citric acid auto combustion method	8.784	6.227	6.223	orthorhombic	0.5, 723-1073	1273/10 and 1573/8	2.4 µm (grain size)	

$BaCe_{0.95}Yb_{0.05}O_{2.975}$	0.13, wet N_2, 923	sol-gel method	8.776	6.219	6.215	orthorhombic	1.4, 723-873	1273/5	75-100 nm (grain size)	[70]
$BaCe_{0.8}Y_xNd0_{.2-x}O_{3-\delta}$	79, (x=0.15), air, 1073	improved Pechini method	*	*	*	orthorhombic	*	1673/10	1-2 μm (grain size)	[76]
$BaCeO_3$: Gd	*	modified Pechini method	8.769	6.243	6.203	orthorhombic	0.54, air, 448-623	1373/4	*	[74]
$BaCeO_3$	*	hydrothermal synthesize by HMTA	8.695	6.231	6.213	orthorhombic	*	1073/10	75 nm (grain size)	[79]
$BaCeO_3$	*	solid-state reaction method	8.786	6.250	6.220	orthorhombic	*	1273	*	[92]
$BaCe_{1-x}Gd_xO_{3-\alpha}$	*	cold crucible direct inductive melting	8.778 (x=0.01)	6.214	6.234	orthorhombic	*	1100/4	*	[93]
$BaCe_{1-x}Y_xO_{3-\alpha}$	*	cold crucible direct inductive melting	4.388 (x=0.05)	-----	-----	cubic	*	1100/4	*	
$BaCe_{1-x}Nd_xO_{3-\alpha}$	*	cold crucible direct inductive melting	8.784 (x=0.1)	6.217	6.232	orthorhombic	*	1100/4	*	

Table 7: The preparation conditions and basic characteristics of powders obtained from different synthesis methods (* - not mentioned in the literature)

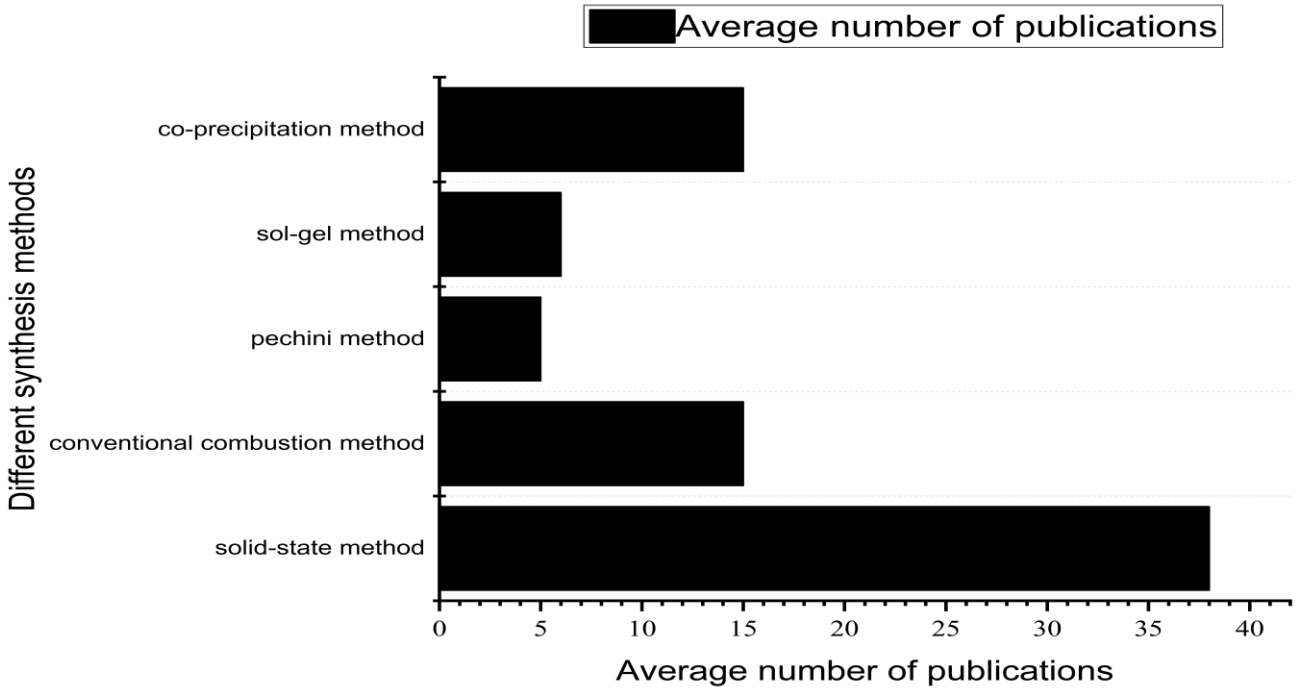

Fig. 2 Average number of publications on different synthesis methods used for BC composite perovskites.

4. Conclusion and future perspectives

In this review, synthesis methods of BC perovskites, including solid-state reaction routes and wet chemical methods with their advantages and weaknesses, are broadly summarized. Fig 2 Shows the average number of publications of BC with different synthesis methods. In the solid-state method, it is somewhat difficult to attain homogeneous composition. It necessitates repeated mixing cycles and heat processing at higher temperatures. The wet chemical methods offer mixing of each component at an atomic level and also decrease the diffusion distance, resulting in the synthesized product with nano crystallite at a lower temperature in comparison with the solid-state method. By choosing appropriate precipitation parameters, the ultrasonic-assisted precipitation method can yield BC perovskite particles of nano crystallite size under relatively lower calcination temperature. In combustion synthesis, the calcination temperature of the samples is within 1173 – 1373 K, and the size of particles is within the range of submicron. Several researchers made various modifications to the combustion process to yield products with great morphology and higher performance. Even though the solid-state method has lots of disadvantages, this is the preferred method of most researchers due to its easiness of processing. Some researchers used other synthesis techniques like the cryogenic method, molten salt method, and hydrothermal synthesis but these are seldom used due to their complexity and multiphase products.

5. Conflicts of Interest

The authors declare no conflicts of interest

6. Acknowledgments

The work has no significant financial support that could have influenced its outcome

7. References

[1] G. Accardo, D. Frattini, and S. P. Yoon, J Alloys Compd **834**, (2020).

[2] M. I. Tenevich, A. P. Shevchik, and V. I. Popkov, J Solgel Sci Technol **101**, 380 (2022).

[3] Z. Khani *et al.*, Chemistry of Materials **22**, 1119 (2010).

[4] (n.d.).

[5] K. Thabet *et al.*, in *Solid Oxide-Based Electrochemical Devices: Advances, Smart Materials and Future Energy Applications* (Elsevier, 2020), pp. 91–122.

[6] J. Jing *et al.*, Chemical Engineering Journal **429**, (2022).

[7] S. A. Sergiienko *et al.*, Ceram Int **43**, 14905 (2017).

[8] F. Deganello, G. Marcì, and G. Deganello, J Eur Ceram Soc **29**, 439 (2009).

[9] P. Diko *et al.*, Journal of the American Ceramic Society **104**, 740 (2021).

[10] A. K. Tyagi, S. v Chavan, and R. D. Purohit, *Visit to the Fascinating World of Nano-Ceramic Powders via Solution-Combustion* (2006).

[11] A. N. Virkar *et al.*, Transactions of the Indian Ceramic Society **41**, 63 (1982).

[12] F. Chen, G. Meng, and D. Peng, *SOLID STATE IONICS Preparation of Nd-Doped Barium Cerate through Different Routes* (1997).

[13] L. Pelletier, A. McFarlan, and N. Maffei, J Power Sources **145**, 262 (2005).

[14] M. Zolkos, International Studies Review **7**, 478 (2005).

[15] K. Przybylski *et al.*, *Chemical Stability Study of Barium Cerate-Based Ionic Conducting Materials* (n.d.).

[16] P. Pulphol *et al.*, Appl Phys A Mater Sci Process **125**, (2019).

[17] I. A. Zvonareva *et al.*, Ceram Int **47**, 26391 (2021).

[18] N. Bonanos *et al.*, *IONIC CONDUCTIVITY OF GADOLINIUM-DOPED BARIUM CERATE PEROVSKITES* (1989).

[19] E. Gorbova *et al.*, J Power Sources **181**, 292 (2008).

[20] B. K. Sonu and E. Sinha, J Alloys Compd **860**, (2021).

[21]) V M Goldschmidt ; ~l *et al.*, *~*) A. WOLD and W. CRor'r* (1926).

[22] S. Yamanaka *et al.*, J Alloys Compd **359**, 109 (2003).

[23] *Ionic Conduction in Perovskite-Type Oxide Solid Solution and Its Application to the Solid Electrolyte Fuel Cell* (Pergamon Press, 1971).

[24] M. Scholten, J. van Miltenburg, and H. Oonk, *Synthesis of Strontium and Barium Cerate and Their Reaction with Carbon Dioxide* (1993).

[25] M. K. Paria and H. S. Maiti, *ELECTRICAL CONDUCTION IN BARIUM CERATE DOPED WITH M203 (M = La, Nd, Ho)* (1984).

[26] H. Iwahara *et al.*, *Proton Conduction in Sintered Oxides Based on BaCe03* (n.d.).

[27] R. C. T. Slade and N. Singh, *Systematic Examination of Hydrogen Ion Conduction in Rare-Earth Doped Barium Cerate Ceramics* (1991).

[28] R. C. T. Slade and N. Singh, *Generation of Charge Carriers and an H/D Isotope Effect in Proton-Conducting Doped Barium Cerate Ceramics* (1991).

[29] K. S. Knight and N. Bonanos, *Crystal Structures of Gadolinium-and Yttrium-Doped Barium Cerate A For* (1992).

[30] T. Scherban *et al.*, *SOLID STATE IOIIICS Raman Scattering Study of Acceptor-Doped BaCeO3* (1993).

[31] T. He, P. Ehrhart, and P. Meuffels, J Appl Phys **79**, 3219 (1996).

[32] S. M. Haile, D. L. West, and J. Campbell, *The Role of Microstructure and Processing on the Proton Conducting Properties of Gadolinium-Doped Barium Cerate* (1998).

[33] W. G. Coors and D. W. Readey, *Proton Conductivity Measurements in Yttrium Barium Cerate by Impedance Spectroscopy* (n.d.).

[34] A. Kruth and J. T. S. Irvine, in *Solid State Ion* (2003), pp. 83–91.

[35] A. McFarlan, L. Pelletier, and N. Maffei, J Electrochem Soc **151**, A930 (2004).

[36] N. Maffei, L. Pelletier, and A. McFarlan, J Power Sources **136**, 24 (2004).

[37] N. Maffei *et al.*, Fuel Cells **7**, 323 (2007).

[38] F. Giannici *et al.*, Chemistry of Materials **19**, 5714 (2007).

[39] J. Dauter *et al.*, J Electrochem Soc **157**, B1413 (2010).

[40] S. S. Bhella *et al.*, Inorg Chem **50**, 6493 (2011).

[41] R. Muccillo, E. N. S. Muccillo, and M. Kleitz, J Eur Ceram Soc **32**, 2311 (2012).

[42] SrZrO, BaCeO, and SrCeO, *Applicability of Gd-Doped BaZrO* (n.d.).

[43] L. Wang *et al.*, Ceram Int **39**, 7959 (2013).

[44] H. Zhou *et al.*, Int J Hydrogen Energy **40**, 8980 (2015).

[45] E. Gorbova *et al.*, Solid State Ion **179**, 887 (2008).

[46] J. Tong *et al.*, Solid State Ion **181**, 1486 (2010).

[47] S. D. Flint and R. C. T. Slade ', *Of Calcium-Doped Barium Cerate Solid Electrolytes Prepared by Different Routes* (1995).

[48] G. Meng *et al.*, *Preparation and Characterization of Barium Cerate-Based Thick Membranes Using a Screen Printing Process* (2000).

[49] P. Kim-Lohsoontorn *et al.*, Chemical Engineering Journal **278**, 13 (2015).

[50] R. Verbová *et al.*, in *Materials Science Forum* (Trans Tech Publications Ltd, 2017), pp. 473–477.

[51] R. Verbov *et al.*, Acta Phys Pol A **133**, 82 (2018).

[52] A. S. Kumar *et al.*, Mater Chem Phys **182**, 520 (2016).

[53] A. S. Kumar *et al.*, Materials Science- Poland **35**, 120 (2017).

[54] M. Irshad *et al.*, Sustainability (Switzerland) **13**, (2021).

[55] R. Gayathri and M. R. Prabhu, Soft Matter **16**, 4220 (2020).

[56] K. Hyun Ryu and S. M. Haile, *Chemical Stability and Proton Conductivity of Doped BaCeO-BaZrO Solid Solutions* (1999).

[57] Q. A. Islam, S. Nag, and R. N. Basu, Ceram Int **39**, 6433 (2013).

[58] D. A. Medvedev *et al.*, Russian Journal of Physical Chemistry A **87**, 270 (2013).

[59] D. Medvedev *et al.*, J Power Sources **221**, 217 (2013).

[60] Y. G. Lyagaeva *et al.*, Physics of the Solid State **57**, 285 (2015).

[61] N. Nasani *et al.*, Int J Hydrogen Energy **38**, 8461 (2013).

[62] K. Gdula-Kasica *et al.*, in *Solid State Ion* (2012), pp. 245–249.

[63] S. Panda *et al.*, J Lumin **214**, (2019).

[64] A. Longo *et al.*, Chemistry of Materials **18**, 5782 (2006).

[65] F. Giannici *et al.*, Solid State Ion **178**, 587 (2007).

[66] H. T. Handal *et al.*, Inorg Chem **55**, 729 (2016).

[67] K. Bae *et al.*, ACS Appl Mater Interfaces **8**, 9097 (2016).

[68] S. Sahani, T. Roy, and Y. Chandra Sharma, J Clean Prod **237**, (2019).

[69] Z. J. Li *et al.*, Sci Technol Adv Mater **8**, 566 (2007).

[70] N. Osman *et al.*, Ionics (Kiel) **14**, 407 (2008).

[71] N. A. Abdullah, S. Hasan, and N. Osman, J Chem (2013).

[72] D. Medvedev *et al.*, Progress in Materials Science **60**, 72 (2014).

[73] V. Agarwal, *Preparation of Barium Cerate-Based Thin Films Using a Modified Pechini Process* (1997).

[74] M. Khandelwal *et al.*, J Eur Ceram Soc **31**, 559 (2011).

[75] X. Deng *et al.*, in *ACM International Conference Proceeding Series* (Association for Computing Machinery, 2019), pp. 250–254.

[76] X. T. Su *et al.*, Solid State Ion **177**, 1041 (2006).

[77] V. O. Igenegbai, R. J. Meyer, and S. Linic, Appl Catal B **230**, 29 (2018).

[78] Z. Khani *et al.*, J Solid State Chem **182**, 790 (2009).

[79] S. Bhowmick *et al.*, Journal of the American Ceramic Society **93**, 4041 (2010).

[80] M. Amsif *et al.*, J Eur Ceram Soc **29**, 131 (2009).

[81] M. Amsif *et al.*, J Power Sources **196**, 3461 (2011).

[82] T. Hibino *et al.*, J Electrochem Soc **149**, A1503 (2002).

[83] G. Ma, T. Shimura, and H. Iwahara, *Ionic Conduction and Nonstoichiometry in Ba Ce Y O* (1998).

[84] W. Suksamai and I. S. Metcalfe, Solid State Ion **178**, 627 (2007).

[85] T. Mori *et al.*, in *Journal of Solid State Electrochemistry* (Springer Science and Business Media, LLC, 2008), pp. 841–849.

[86] D. W. Lee, J. H. Won, and K. B. Shim, Mater Lett **57**, 3346 (2003).

[87] *PREPARATION AND PROPERTIES OF FINE BaCeO* (n.d.).

[88] S. B. C. Duval *et al.*, Solid State Ion **178**, 1437 (2007).

[89] G. Accardo *et al.*, Ceram Int **45**, 9348 (2019).

[90] L. Spiridigliozzi *et al.*, Ceram Int **45**, 4570 (2019).

[91] E. Gorbova *et al.*, J Power Sources **181**, 207 (2008).

[92] S. Yamanaka *et al.*, J Alloys Compd **359**, 1 (2003).

[93] B.-T. Melekh *et al.*, *Structure, Phase Transitions and Optical Properties of Pure and Rare Earth Doped BaCeO , SrCeO Prepared by Inductive Melting 3 3* (1997).